ELSEVIER

Journal of Chromatography A, 825 (1998) 55–69

JOURNAL OF CHROMATOGRAPHY A

Capillary zone electrophoresis at subzero temperatures III. Operating conditions and separation efficiency

Stacey Ma[1], Csaba Horváth*

Department of Chemical Engineering, Mason Laboratory, Yale University, P.O. Box 208286, New Haven, CT 06520-8286, USA

Received 8 December 1997; received in revised form 31 July 1998; accepted 18 August 1998

Abstract

The advantages of carrying out capillary zone electrophoresis at subambient rather than ambient temperatures are examined. They include the possibility of using higher electric field strength and/or buffer concentration as well as wider capillary lumen without untoward effects of Joule heating on the separation. Furthermore, the separation efficiency is enhanced as molecular diffusivity decreases with temperature. A Beckman P/ACE unit with an auxiliary cooling system was used at temperatures down to −20°C and, based on the dependence of axial temperature gradient on the capillary length and the temperature of the coolant, an average capillary temperature was defined. The day-to-day migration times of proteins were reproducible with an R.S.D. better than 2.3%. The improvements in the separation efficiency upon lowering the temperature from 40 to 1°C are illustrated by the electropherograms of four closely related peptides. Generally, the plate efficiency is enhanced at low temperatures and the analysis time is prolonged due to the increased viscosity. However, the current at a fixed electric field also decreases with temperature and the capillary can be shortened to speed up the analysis. With benzenesulfonic acids, the rate of the generation of theoretical plates was two- to three-times higher using a 27 cm long capillary at −15°C than a 47 cm long capillary at 40°C. By using a 180 μm instead of a 50 μm I.D. capillary for the separation of the four peptides, the sample loading could be increased about 15 times without loss of resolution. In the capillary zone electrophoresis of proteins, it was found that protein interactions with the capillary wall can be significantly reduced by increasing buffer concentration at low temperatures where salt mediated hydrophobic interactions are attenuated. This is illustrated by the separation of β-lactoglobulins A and B in a raw fused-silica capillary using 400 m*M* sodium borate buffer, pH 8.4. The results suggest that at subambient or even subzero temperatures, the scope of CZE can be extended by several ways so that the benefits are great enough to justify the use of a cooling system and temperature control appropriate for psychroelectrophoresis with fused-silica capillaries.

Keywords: Temperature effects; Efficiency; Peptides; Benzensulfonic acids; Proteins

1. Introduction

Temperature is a convenient and highly effective operational variable in many separation processes. In high-performance liquid chromatography (HPLC) elevated temperatures [1–4] up to 120°C have been shown to offer enhanced speed and efficiency of analysis. In capillary zone electrophoresis (CZE), untoward bubble formation, deterioration of the separation efficiency and degradation of unstable sample components can be reduced when operating the capillary at subambient temperatures [5,6]. In

*Corresponding author.

[1]Present address: Department of Analytical Chemistry, Genentech Inc., South San Francisco, CA 94080, USA.

0021-9673/98/$ – see front matter
PII: S0021-9673(98)00680-3

contradistinction, capillary electrochromatography (CEC), like other chromatographic methods, might benefit from the employment of elevated temperatures due to the reduced viscosity and the concomitant enhancement of mass transfer. Yet, HPLC, CZE and CEC are performed mostly at ambient temperature.

Tiselius [7] carried out already in the late 1930s electrophoresis in the absence of an anticonvective medium at 4°C, where the density of water is maximum, in order to minimize convective mixing due to temperature gradients. In the 1970s, gel electrofocusing in glass tubes was used at −10°C [8] in order to study the interaction of hemoglobin with various ligands at a temperature low enough for the complexes to be stable. Furthermore, the investigation of thermally unstable intermediates of hemoglobin during oxidation [9] was carried out at −25°C by slab gel electrophoresis. More recently, slab-gel electrophoresis was used at 4°C [10] in the study of lipopolysaccharides in order to prevent the partial decomposition of fatty acid esters. Very recently, poly(ethylene glycol)methacrylate–acrylamide copolymer gel, which is stable at low temperatures [11] was introduced to facilitate slab gel electrophoresis at low temperatures. It was found that upon lowering the temperature from 25 to −20°C, the applied voltage could be increased without loss of resolution due to excess Joule heating and as a result the speed of a typical electrophoretic run was increased by a factor of eight.

In the modern era of CZE, the potential advantages of low temperature, e.g., enhanced efficiency, selectivity and speed, have received little attention and temperature control in CZE, just as in HPLC, serves mainly to enhance reproducibility of the measurements. Even the highly sophisticated commercial CZE instruments are only equipped to control the temperature of the capillary from a few degrees below ambient to about 50 to 70°C. Nonetheless, with a specially altered instrument, the advantages of CZE at subambient or even subzero temperatures were explored in a few instances. The separation of heterocyclic nitrosoamino acid conformers was greatly improved at 5°C as compared to room temperature [12] using a modified P/ACE unit (Beckman, Fullerton, CA, USA). For the separation of four local anesthetics at 10°C [13], a Peltier-based cooling system was employed for thermostatting the capillary in a commercial SpectraPhoresis unit (ThermoSeparations, CA, USA). In our laboratory, the employment of subzero temperatures for the CZE separation of various isomers, such as the *cis–trans* conformers of small peptides containing peptidyl–proline bond [5] and the enantiomers of biogenic amines [6] was carried out with a modified Beckman P/ACE unit at temperatures as low as −20°C.

The goals of this study are to examine the benefits and the problems associated with CZE at low temperatures that is conveniently referred to as psychroelectrophoresis from the Greek word psÿchrós for wet cold. Particular attention is paid to the benefits arising from the increase in viscosity and the experimental results are discussed in the light of the theoretical predictions.

2. Experimental

2.1. Chemicals

N-Acetylphenylalanine (F) and peptides, phenylalanyl-leucine (FL), phenylalanyl-tyrosine (FY), phenylalanyl-alanine (FA), glycyl-phenylalanine (GF), phenylalanyl-glycine (FG), glycyl-glycyl-phenylalanine (GGF) and phenylalanyl-glycyl-glycine (FGG) as well as proteins, myoglobin, β-lactoglobulin and purified β-lactoglobulin A and β-lactoglobulin B, were purchased from Sigma (St. Louis, MO, USA). Tyrosinyl-aminoisobutyl-phenylalanyl-aspartyl-valyl-valyl-glycine (F-Aib-FDVVG) was donated by Laboratory of Chemical Biology and Peptide Research (Clinical Research Institute of Montreal, Montreal, Canada). Trimethylphenylammonium iodide (TMP) was supplied by ChemService (West Chester, PA, USA). Benzenesulfonic acid (sodium salt), 1,2-benzenesulfonic acid (dipotassium salt), 1,3-benzenesulfonic acid (disodium salt) as well as acrylamide and optically pure biogenic amine, L-ephedrine, were purchased from Aldrich (Milwaukee, WI, USA). The trisodium salt of 1,3,5-benzenetrisulfonic acid was obtained from Eastman Kodak (Rochester, NY, USA).

Reagent grade phosphoric acid, sodium hydroxide and HPLC grade acetonitrile were supplied by Fisher (Pittsburgh, PA, USA), sodium borate ($Na_2B_4O_7\cdot$

$10H_2O$) by Mallinckrodt (Paris, KY, USA), boric acid and anhydrous glycerol by J.T. Baker (Phillipsburg, NJ, USA). Buffer standards, potassium hydrogenphthalate, pH 4.01, and potassium phosphate, pH 7.00, were from Baker and potassium carbonate, pH 10.00, was from Brand-Nu Labs. (Meriden, CT, USA). Deionized water was prepared by the Nano-Pure purification system from Barnstead (Boston, MA, USA) and used throughout the experiments.

2.2. Buffers

In most cases, solutions containing 50 m*M* sodium phosphate in water–acetonitrile (63:35, v/v) were used and the apparent pH* of the hydro–organic solutions was measured with the glass electrode and adjusted with 1 *M* NaOH to 2.5. In studies with varying capillary inner diameter, 25 m*M* sodium phosphate solution in water–glycerol (63:35, v/v), pH* 7.0, was used. The freezing points of both buffers were about −20°C [14]. A stock of 400 m*M* sodium borate buffer, pH 8.4, was prepared by adding 400 m*M* boric acid to 100 m*M* sodium tetraborate solutions to reach the desired pH. By serial dilution of this buffer, we obtained 200, 100, 50 and 25 m*M* sodium borate solutions and the pH of each buffer was adjusted their pH with boric acid of that particular concentration. This set of sodium borate buffers of various concentration was used to investigate the effect of the buffer concentration. All buffers were prepared and their pH values reported here were measured at room temperature.

2.3. Instrumentation

A Model P/ACE 2200 capillary electrophoresis unit (Beckman) was adapted for psychroelectrophoresis and the flow sheet of the modified cooling system is shown in Fig. 1. A Model RTE-4DD thermostatted refrigerated circulating bath (Neslab, Portsmouth, NH, USA) with ethylene glycol as the coolant was used to assist the original cooling system of the instrument. The original lines of P/ACE coolant circulation were relocated and insulated with glass wool. Its operational part is illustrated with dashed line in Fig. 1. The original temperature control unit was bypassed so that the coolant circulation was directed through a 350 cm long copper heat

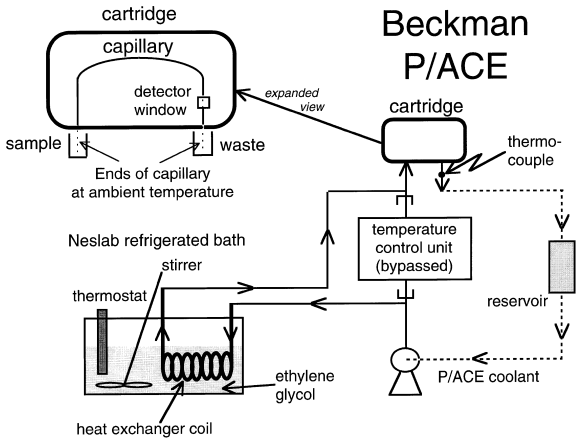

Fig. 1. Schematically illustration of the P/ACE CZE unit modified for psychroelectrophoresis. An auxiliary cooling system is used to assist temperature control down to −20°C. The original lines of the circulating coolant are relocated, connected to an heat exchange coil and insulated with glass wool. The coolant temperature is measured by the thermocouple at the coolant outlet of the cartridge. The axial temperature nonuniformity of the capillary is illustrated in the expanded view where the sections of the capillary that are at the ambient temperature, including the ends and the detection window, are shown in dashed line.

exchanger with an O.D. and I.D. of 3/8 in. and 3/16 in., respectively (1 in.=2.54 cm). The heat exchanger coil is placed in the Neslab bath as illustrated by dotted line in Fig. 1. The temperature of the coolant was measured at the outlet of the cartridge, as shown in Fig. 1, by a Model DP116-TC2 thermocouple from Omega (Stamford, CT, USA) with a precision of 0.1°C. The original temperature control unit in the P/ACE was bypassed and the coolant temperature was controlled by the thermostat setting of the external refrigerated bath. As a result of a small increase in temperature due to the environment, the temperature of the external bath was set at a lower value than the thermocouple reading. A PowerMate SX/20 from NEC Technologies (Boxborough, MA, USA) with P/ACE 2000 Series Microsoft for Windows version 3.0 from Beckman was used for the control of the instrument and data processing.

2.4. Capillary zone electrophoresis

Polyimide cladded fused-silica capillaries of 375 μm O.D. and 50 μm or 180 μm I.D. were obtained

from Quadrex (New Haven, CT, USA) and used in lengths ranging from 27 to 87 cm. A 2 to 3 mm section of the polyimide outer coating was burned off to make a window for the UV–Vis detector of the P/ACE 2200 CZE unit that was set at 214 nm throughout the experiments.

In most cases, sample components were dissolved in the appropriate running buffer at a concentration of approximately 0.3 mg/ml. In studies on the effect of buffer concentration, the samples were dissolved in water to benefit from stacking. The samples were injected by applying 3448 N/m^2 N_2 pressure for 2 to 10 s depending on the temperature. Between runs the capillary was flushed with at least five column volumes of the running buffer at an inlet pressure of $1.379 \cdot 10^5$ N/m^2.

3. Results and discussion

3.1. Temperature dependence of the operational parameters

3.1.1. Electrophoretic mobility

The electroosmotic flow (EOF) velocity is measured by an inert marker of which mobility, μ_{EOF}, is expressed by the Helmholtz–Smoluchowski equation [15,16] as

$$\mu_{EOF} = \frac{\varepsilon\varepsilon_0\zeta}{\eta} \quad (1)$$

where ε_0 is the permittivity of the vacuum, ζ is the zeta potential at the inner wall of the capillary, ε and η are the respective dielectric constant and viscosity of the medium.

The electrophoretic mobility of a migrant, μ, if its molecular size is small compared to the double layer thickness, is given by Henry's equation [15,16] as

$$\mu = \frac{2\varepsilon\varepsilon_0\zeta_a}{3\eta} \quad (2)$$

where ζ_a is the zeta potential of the migrant. For a nonconducting sphere with a uniform surface charge, Eq. (2) becomes

$$\mu = \frac{ze}{6\pi\eta r_{st}} \quad (3)$$

where z is the characteristic charge and r_{st} is the hydrodynamic (Stokes) radius.

The mobilities of the migrants and background ions are expected to change with temperature mainly due to changes in the viscosity of the medium. Under the experimental conditions used in this study, the temperature dependence of the viscosity, η, can be described by the Andrade equation [17] as

$$\eta = A\exp\left(\frac{B}{T}\right) \quad (4)$$

where A and B are empirical constants for a given liquid and T is the absolute temperature.

As the heat of ionization of phosphate or borate buffers used in this study is close to zero [14], the changes in the pH values of the background electrolytes (BGEs) are assumed to be negligible. In addition, if the zeta potential, the molecular charge and the dielectric constant are assumed to be temperature independent, then in view of Eqs. (2)–(4), the dependence of the electrophoretic mobility, μ, on the temperature is given by

$$\ln \mu = A_m - \frac{B}{T} \quad (5)$$

where constant A_m reflects the dielectric properties of the buffer and the molecular properties of the component of interest. The other empirical constant B is determined only by the properties of the buffer.

The temperature dependence of μ_{EOF} can be expressed in an analogous fashion as

$$\ln \mu_{EOF} = A_{EOF} - \frac{B}{T} \quad (6)$$

where A_{EOF} depends on the dielectric properties of the buffer and the zeta potential of the capillary inner surface and is taken as a constant in most cases.

3.1.2. Current

According to Ohm's law, the current, I, is given by

$$I = \frac{\kappa_e A_c V}{L} = \kappa_e A_c E \quad (7)$$

where κ_e is the conductivity of the BGE, V is the applied voltage, E is the electric field strength, A_c and L are the respective cross sectional area of the lumen and the length of the capillary. The con-

ductivity, κ_e, is determined by the mobility, μ_i, and concentration, c_i, of various ions, i, in the BGE [18] as

$$\kappa_e = \sum_i z_i F c_i \mu_i \quad (8)$$

where F is the Faraday constant and z_i is the charge on the ion i.

The mobilities of the background ions change with the temperature mainly due to changes in the viscosity of the medium. Thus, the temperature dependence of conductivity can be expressed by combining Eqs. (5) and (8) as

$$\ln \kappa_e = A_k - \frac{B}{T} \quad (9)$$

where A_k is determined by the ionic strength and the molecular dimensions of the ions in that particular BGE and hence it may also considered to be constant under typical experimental conditions. According to Eqs. (5), (6), (9), the plots of the logarithmic electrophoretic mobility, μ_{EOF} and conductivity against the reciprocal temperature are linear and the slopes are largely determined by changes in the viscosity of the electrophoretic medium.

In order to test Eqs. (6) and (9), values of μ_{EOF} and κ_e were measured in 100 m*M* neat aqueous borate, pH 8.4, as well as in 50 m*M* borate buffer containing 23% (v/v) glycerol, pH* 11.3. The results are plotted in Fig. 2 against the reciprocal temperature in the range from 1 to 50°C (dashed lines) and from −17 to 40°C (solid lines), respectively. Since all plots are linear with correlation coefficients better than 0.99 and the two pairs of lines representing dependence of the mobility and conductivity on the reciprocal temperature in the same medium have almost identical slopes, the data lends strong support to both Eqs. (6) and (9). The slopes thus obtained, together with the slopes of similar plots for the other three buffers used in this study, are listed in Table 1. For parameter B in neat aqueous buffers containing different borate concentrations, we obtain values ranging from 1820–1862 K that closely brackets the literature value of 1844 K measured with water [14]. With aqueous solutions containing 23% and 35% glycerol, the average values of parameter B, based on the measured mobility and conductivity data, were

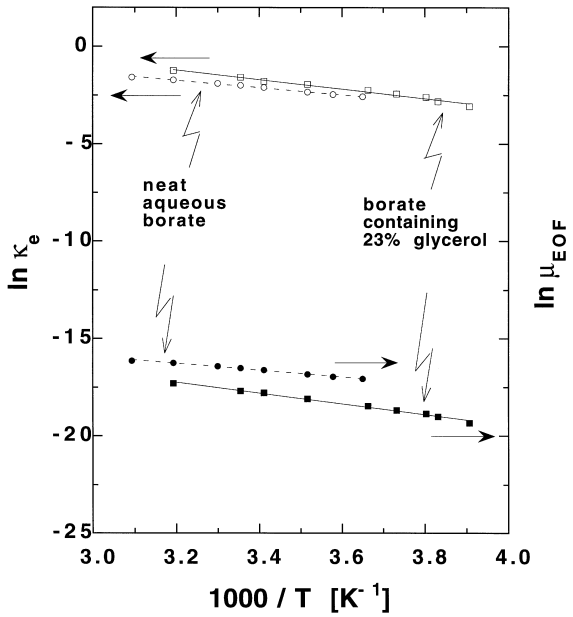

Fig. 2. Plots of the logarithmic conductivity, ln κ_e, of the medium (open symbols) and the logarithmic mobility, ln μ_{EOF}, of the EOF tracer acrylamide (solid symbols) against the reciprocal absolute temperature. Temperature ranges from 1 to 50°C, neat aqueous 100 m*M* sodium borate buffer, pH 8.4 (circles); from −17 to 40°C, 50 m*M* sodium borate in water–glycerol (77:23, v/v), pH* 11.3 (squares). Other conditions: fused-silica capillary, 37 cm (effective length 30 cm)×50 μm I.D.; applied voltage, 30 kV.

found to be respectively, 2610 K and 2960 K that are significantly higher than those with neat aqueous borate buffer. In the literature [19], the respective viscosities of neat water and the solutions containing 23% (v/v) and 35% (v/v) glycerol are 1.0, 1.9 and 3.0 cp at 20°C. This finding is consistent with the Lewis–Squires postulate [20], that the sensitivity of viscosity of liquids to temperature change depends primarily on the magnitude of the viscosity. Consequently, the higher the viscosity of the liquid, the greater is the effect of changing temperature on its viscosity as measured by parameter B.

3.2. Temperature profile in the capillary

As shown in Fig. 1, the capillary is thermostatted by the coolant circulating inside of the cartridge of the Beckman P/ACE unit. In the arrangement used, about a 4 cm long segment is exposed to ambient temperature at each end of the capillary. As a result,

Table 1
Experimental values of parameter B for the temperature dependence of EOF and conductivity according to Eqs. (6) and (9), respectively

Electrophoretic medium	Parameter B (K) evaluated from		
	Mobility of EOF tracer	Conductivity	Viscosity[a]
100 m*M* sodium borate, pH 8.4	1820	1858	1844
200 m*M* sodium borate, pH 8.4	1834	1846	1844
400 m*M* sodium borate, pH 8.4	1826	1862	1844
50 m*M* sodium borate in water–glycerol (77:23, v/v), pH* 11.4	2449	2771	–
25 m*M* sodium phosphate in water–glycerol (65:35, v/v), pH* 7.0	3300	2621	–

Also listed is the literature value of parameter B for neat water. Raw fused-silica capillary, 37 cm (effective length 30 cm)×50 μm I.D.; applied voltage, 30 kV.
[a] Data for neat water in the temperature range from 0 to 100°C [14].

there is an axial temperature gradient in the capillary when the coolant temperature is other than ambient. In order to make a crude estimate of the axial temperature profiles, let us assume that the temperature of that part of the capillary which is in contact with the coolant, has the same temperature as the coolant and conduction is the only mode of heat transfer along the capillary tube. In Fig. 3, axial temperature profiles in capillaries of varying lengths are schematically illustrated by using the dimensionless axial position that is given by the ratio of the distance into the capillary, L_x, and the total length of the capillary, L. As seen in Fig. 3, with the 27 cm, 47 cm and 87 cm long capillaries the fractional tube lengths of 19 cm, 39 cm and 79 cm are at the coolant temperature. This reflects that due to instrumental constraints the thermal entrance length and consequently the axial nonuniformity is larger with the 27 cm long capillary but negligible with the 87 cm long capillary.

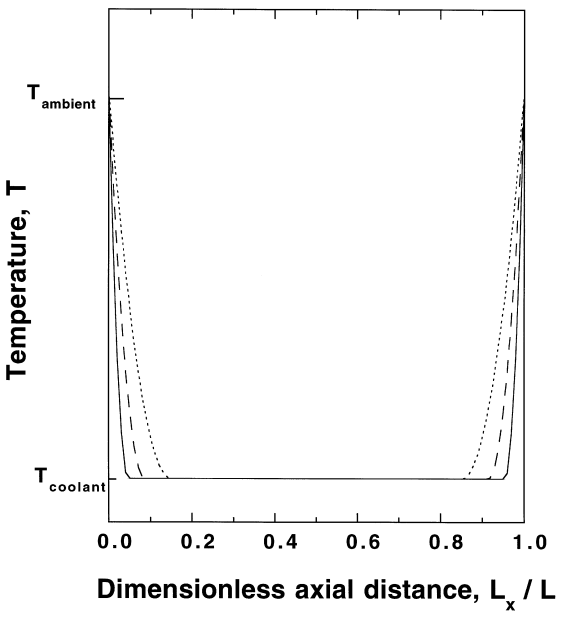

Fig. 3. Estimated axial temperature profiles in capillaries of different lengths housed in the cartridge. The dimensionless axial position is L_x/L, T_{amb} is the ambient temperature and T_{set} is the coolant temperature. $L=87$ cm (solid line); $L=47$ cm (dashed line) and $L=27$ cm (dotted line).

Experimental support for the predicted axial temperature gradients comes from the apparent electrophoretic mobilities of *N*-acetylphenylalanine, phenylalanyl-alanine and phenylalanyl-glycyl-glycine that were evaluated from their electrophoretic migration times in 27, 47 and 87 cm long capillaries under arheic conditions, i.e., in the absence of EOF since the mobility of acrylamide, the EOF tracer was practically zero. To avoid excess Joule heating, all measurements were carried out at constant power of 0.08 W. The BGE was 50 m*M* sodium phosphate in water–acetonitrile (65:35, v/v), pH* 2.5. To avoid temperature disturbances inside the capillary due to sample introduction, the samples were thermally equilibrated at the experimental capillary temperature prior to injection. The mobility data thus obtained are plotted against the capillary length in Fig. 4. It is seen that at 25°C the mobilities of the three probes are only weakly dependent on the capillary length. However, at 7.1°C and −15.7°C, all apparent mobilities decrease upon increasing the length of the capillary due to the greater temperature nonuniformity in shorter capillaries.

In order to estimate the temperature in capillaries with significant axial thermal nonuniformities, let us

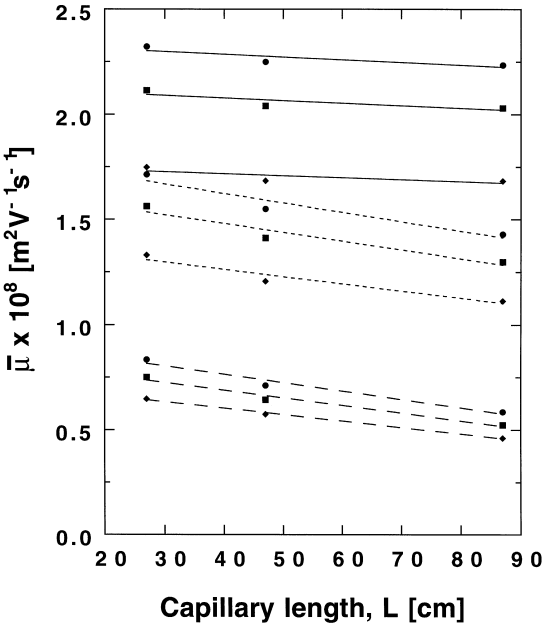

Fig. 4. Plots of the measured electrophoretic mobility against the total length of the capillary. Samples: (●) FA; (■) FGG and (♦) F. Temperature: 25°C (solid line); 7.1°C (dotted line) and −15.7°C (dashed line). Conditions: 50 μm I.D. fused-silica capillaries of different lengths; 50 m*M* sodium phosphate in water–acetonitrile (65:35, v/v), pH* 2.4; constant power, 0.08 W.

define an average temperature based on the apparent electrophoretic mobility of an appropriate migrant. Assuming that in two capillaries of different lengths, the ratio of apparent mobilities calculated from the migration time under arheic condition depends on the corresponding average temperatures [21–23], we can write in view of Eq. (5) that

$$\ln \frac{\bar{\mu}_1}{\bar{\mu}_2} = -B\left(\frac{1}{\bar{T}_1} - \frac{1}{\bar{T}_2}\right) \tag{10}$$

where parameter B is the empirical constant in Eq. (4), $\bar{\mu}_1$ and $\bar{\mu}_2$ are the apparent electrophoretic mobilities measured at the respective average temperatures $\bar{T}_1$ and $\bar{T}_2$. If the apparent electrophoretic mobility of a migrant measured in a 87 cm long capillary is $\bar{\mu}_1$ at capillary temperature $\bar{T}_1$, then from the apparent electrophoretic mobility of the same migrant measured in a shorter capillary, $\bar{\mu}_2$, by rearranging Eq. (11) the average temperature $\bar{T}_2$ in the shorter capillary can be estimated as

$$\bar{T}_2 = \frac{1}{\dfrac{1}{\bar{T}_1} + \dfrac{\ln \bar{\mu}_1 - \ln \bar{\mu}_2}{B}} \tag{11}$$

As mentioned earlier, parameter B is determined for a particular medium from the mobility of suitable probes or the conductivity at various temperatures. In this case, parameter B was determined from the mobilities measured under conditions stated in Fig. 4. It is important to recall that the temperature is assumed to be uniform in the 87 cm long capillary and equal to the coolant temperature as measured by the thermocouple so that the apparent electrophoretic mobility is the true mobility of the probe at that temperature. By plotting the logarithmic mobilities of a migrant measured in the 87 cm long capillary against the reciprocal absolute temperatures according to Eq. (5), we obtained three straight lines for the three probes used here with a linear regression coefficients better than 0.99 for all cases (data not shown). Based on the three slopes, an average value of 2527 K was obtained for parameter B with 50 m*M* sodium phosphate in water–acetonitrile (65:35, v/v), pH* 2.4, as the BGE.

Once the value of parameter B is determined, the average temperatures in the 27 cm and 47 cm long capillaries can be estimated using Eq. (11). As expected and seen from Table 2, at 25°C the temperature gradients in the 27 as well as the 47 cm long capillary are rather small so that the average temperatures in both capillaries are within 1.5°C of

Table 2
List of the average temperatures, $\bar{T}$, in 27, 47 and 87 cm long capillaries at three settings of the coolant temperature, T_c

Capillary length, L (cm)	Temperature					
	$T_{c,1}$ at −15.7°C		$T_{c,2}$ at 7.1°C		$T_{c,3}$ at 25.0°C	
	$\bar{T}_1$	$\Delta\bar{T}_1$	$\bar{T}_2$	$\Delta\bar{T}_2$	$\bar{T}_3$	$\Delta\bar{T}_3$
27	−6.2	9.5	12.8	5.7	26.4	1.4
47	−10.2	5.5	9.7	2.6	25.2	0.2
87	−15.7	0	7.1	0	25.0	0

The differences between the average capillary temperatures and the coolant temperatures (as measured with the 87 cm capillary) are also listed under ΔT. The average capillary temperatures were calculated from the apparent electrophoretic mobilities according to Eq. (12). Capillaries, various lengths of 50 μm I.D.; 50 m*M* sodium phosphate in water–acetonitrile (65:35, v/v), pH* 2.5; power, 0.08 W; temperature, 25°C.

the coolant temperature. At 7°C, however, the average temperatures inside the 47 and the 27 cm long capillaries are different by 3 or 6°C from the coolant temperature, respectively. The deviation is even more pronounced at −15.7°C, where the respective average temperatures were found to be almost 10 and 6°C higher than the coolant temperature.

In order to assess the reproducibility of CZE at low temperatures, a set of eight model compounds including small amines, peptides and proteins were subjected to CZE at 4°C. The relative standard deviation (R.S.D.) of the measured migration times was determined and the results are listed in Table 3. The data shows that the run-to-run R.S.D. is better than 0.6% based on four consecutive runs; whereas the day-to-day variability is better than 2.3% on three consecutive days. Although, the results indicate that CZE has a potential as a high-performance analytical technique even at low temperatures, a caveat is in place due to the axial temperature nonuniformity in the CZE capillary at subambient temperatures. Further improvements in instrument design are required to provide conditions for uniform capillary temperature even when it is far from ambient.

Table 3
Reproducibility of migration times in the CZE of various compounds at 4°C

Compound	R.S.D. (%)			
	Run-to-run			Day-to-day
	24°C	22°C	21°C	
Acrylamide	0.15	0.30	0.53	1.67
TMP[a]	0.23	0.23	0.45	1.59
Ephedrine	0.06	0.27	0.41	1.52
GGF[b]	0.29	0.34	0.23	2.10
F[c]	0.56	0.10	0.10	2.25
Myoglobin	0.34	0.54	0.24	1.81
β-Lactoglobulin A	0.47	0.27	0.13	2.25
β-Lactoglobulin B	0.48	0.21	0.11	2.20

Capillary, 37 cm (effective length 30 cm)×50 μm; buffer, 400 m*M* sodium borate, pH 8.4; applied voltage, 25 kV; current, 74 μA. The capillary was rinsed with five column volumes of water, 0.1 *M* NaOH, water and finally of the running buffer. The capillary was equilibrated at 4°C for at least 5 min before each run.

[a] Trimethylphenylammonium iodide.

[b] Glycyl-glycyl-phenylalanine.

[c] *N*-Acetylphenylalanine.

3.3. Advantages of CZE at low temperatures

3.3.1. Plate efficiency

In ideal CZE, peak broadening is solely due to longitudinal molecular diffusion. Under arheic conditions, the peak efficiency [24,25] in terms of plate number, *N*, is independent of the capillary length and given by

$$N = \frac{\mu V}{2D_m} \tag{12}$$

where D_m is the molecular diffusion coefficient of the migrant under investigation and it is described by [24,25],

$$D_m = \frac{RT}{N_A 6\pi\eta r_{st}} \tag{13}$$

where R is the gas constant and N_A is the Avogadro's number. By combining Eqs. (3), (12), (13), we obtain [24,25],

$$N = \frac{zFV}{2RT} \tag{14}$$

According to Eq. (14), the plate efficiency is directly proportional to the applied voltage and molecular charge and inversely proportional to the temperature. The effect of temperature on the separation efficiency is illustrated in Fig. 5 by electropherograms of four peptides having molecular charges close to one under the conditions investigated here. According to Eq. (14), the improvement on the separation efficiency is expected to be about 15% upon reducing the temperature from 40 to 1°C. It is seen from Fig. 5 that the separation efficiency of the four peptides indeed improved upon lowering the temperature. Moreover, for peptides Phe–Leu (1) and Tyr–Aib–Phe–Asp–Val–Val–Gly (2), the improvement in their overall resolution is even greater than the theoretical prediction on the enhancement of efficiency alone and therefore is attributed to the concomitant enhancement in the selectivity upon lowering the separation temperature.

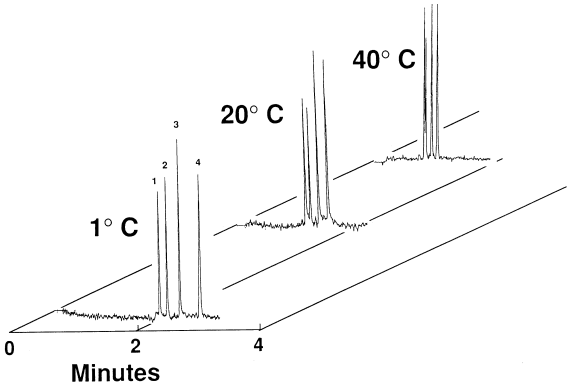

Fig. 5. Electropherograms of peptides obtained at temperatures 1, 20 and 40°C. Capillary, 37 cm (effective length 30 cm)×50 μm I.D.; 100 m*M* sodium borate, pH 8.4; applied voltage, 30 kV; current in the order of increasing temperature, 12, 20 and 29 μA. Sample components: 1=FL; 2=Y-Aib-FDVVG; 3=FY; 4=F.

3.3.2. Rate of plate generation

In addition to the plate efficiency and selectivity, the speed of analysis is another measure that should be taken into account in evaluating the overall separation efficiency in CZE. The time of analysis is expressed by the migration time, *t*, it is related to the electrophoretic mobility of the component of interest by

$$t = \frac{lL}{\mu V} \tag{15}$$

where *l* is the migration distance from the inlet to the detection point.

By combining Eqs. (3), (14), (15) we obtain for the rate of plate generation, N/t, the following expression [24,25],

$$\frac{N}{t} = \frac{z^2 eFV^2}{12\pi R\eta r_{st} TlL} \tag{16}$$

The rate of plate generation for a molecule with unit charge and a Stokes radius of 10 Å in capillaries of different lengths was calculated for an aqueous medium using Eq. (16). The results are shown in Fig. 6 and illustrate that the rate of plate generation decreases with temperature as a result of increasing viscosity as predicted in the literature [24]. However, upon lowering the temperature, the current also decreases due to the higher viscosity. Therefore, when lowering the temperature, the capillary length can be reduced, within the limits of permissible Joule heating as well as instrument design, to avoid the loss of separation speed. For instance, it can be seen in Fig. 6 that the N/t values for a 27 cm long capillary (the shortest length possible in the Beckman P/ACE unit) are greater than those for a 47 cm long capillary at all temperatures while keeping the applied voltage constant.

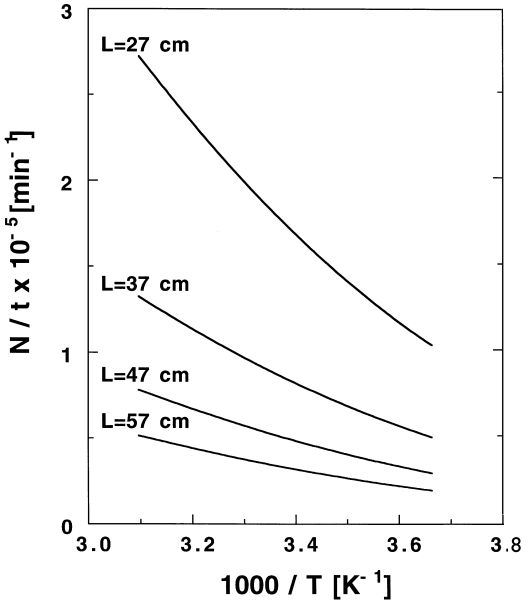

Fig. 6. Rate of plate generation as a function of the reciprocal temperature with the capillary of length as the parameter according to Eq. (16). The viscosity of water in the temperature range from 0 to 50°C was used and $z=1$, $r_{st}=10$ Å, and $V=30$ kV.

In order to further examine this experimentally, four benzenesulfonic acids were separated at two different temperatures with two capillaries having different lengths. In both cases, the applied voltage and the buffer were the same and the resulting electropherograms are shown in Fig. 7. The four acids were resolved at baseline in less than 4 min at −15°C with the 27 cm long capillary as seen in Fig. 7a and they were also separated with baseline resolution in about 4 min with the 47 cm capillary at 40°C as seen in Fig. 7b. However, the plate efficiencies are significantly higher at −15°C as indicated by the sharp peaks. From the two electropherograms, the ratios of the migration times, the number of theoretical plates and the rate of plate generation, which express the speed and efficiency of the

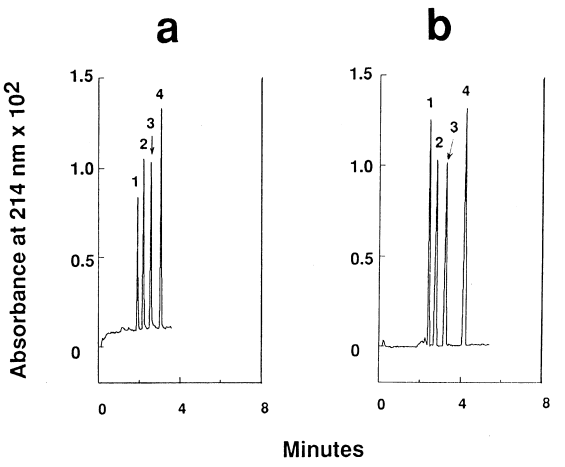

Fig. 7. Electropherograms of benzene sulfonic acids obtained at (a) −15°C and (b) 40°C with columns of 27 cm (effective length 20 cm) and 47 cm (effective length 40 cm), respectively. Peaks: 1=benzenetrisulfonic acid; 2=1,3-benzenesulfonic acid; 3=1,2-benzenesulfonic acid; 4=benzenesulfonic acid. Capillaries, 50 μm I.D. of different lengths; 50 m*M* sodium phosphate in water–acetonitrile (65:35, v/v), pH* 2.4; applied voltage, 25 kV and current: (a) 22 μA; (b) 27 μA.

separation, were determined and listed in Table 4. Comparison of the ratios shows that at low temperatures the speed of the separation is not compromised and the efficiency is higher when using the shorter capillary. Under the conditions investigated here, the ratio of plates/time, N/t, is calculated to be about 3 according to Eq. (16) assuming that changes only occurred in the viscosity, the separation temperature and the capillary length. It is seen from Table 4 that the values of N/t are slightly below 3, with the exception of benzenetrisulfonic acid (BTSA), as expected since the value of 3 is calculated under ideal conditions. However, the improvement on the rates of plate generation is significantly lower for BTSA at a value of only 1.8. Moreover, the ratio of the separation efficiencies, N_a/N_b, and migration times, t_a/t_b, are expected to be about 1.2 and 0.35, respectively according to Eqs. (14) and (15) for the conditions studied here under the above mentioned assumptions. In comparison, the experimental values obtained are quite different from the theoretical predictions. For the separation speed, the values are all greater than 0.35 ranging from 0.702 to 0.756 and hence the improvement on the separation speed with a shorter capillary at lower temperature is less than ideal under the conditions studied here. On the other hand, the improvement on the plate efficiencies with values ranging from 1.33 to 2.03 are greater than the theoretical prediction. The discrepancies observed here clearly indicate that for the benzenesulfonic acids studied here in a hydro–organic medium, there are changes in their intrinsic molecular properties, i.e., molecular charge and/or hydrodynamic size, that result in the deviation from these theoretical predictions. Nevertheless, in this case, these changes result in greater enhancement in the overall separation efficiencies and the rates of plate generation. This finding clearly suggests that temperature may play a key role in improving the separation by manipulating various molecular properties of certain molecules in CE systems other than those involves reactions and/or interactions that already being reported earlier [5,6,8,10,12].

3.3.3. Capillary inner diameter

In CZE, at otherwise identical conditions, the current increases with the squared inner diameter of

Table 4
Ratios of the migration times, plate efficiencies and rates of plate generation measured with a 27 cm long capillary at −15°C (a) and a 47 cm long capillary at 40°C (b) in the CZE of benzenesulfonic acids under arheic conditions

Migrant	Ratios of		
	Migration times t_a/t_b	Plate efficiencies N_a/N_b	Plates/time $(N/t)_a/(N/t)_b$
Benzenesulfonic acid	0.702	2.03	2.90
1,2-Benzenedisulfonic acid, dipotassium salt	0.756	1.76	2.33
1,3-Benzenedisulfonic acid, disodium salt	0.754	1.75	2.32
Benzenetrisulfonic acid	0.738	1.33	1.80

Capillary, 50 μm I.D.; 50 m*M* sodium phosphate in water–acetonitrile (65:35, v/v), pH* 2.5; applied voltage, 25 kV; current, (a) 22 μA and (b) 27 μA.

the capillary. Therefore, in order to avoid problems arising from excess Joule heating, capillaries having greater than 100 μm inner diameter are seldom used despite the many advantages of the greater capillary lumen. For instance, the sensitivity with on-column detection improves with increasing inner diameter of the capillary and the interference by untoward interactions with the capillary inner wall are attenuated as the result of the reduced surface to volume ratio. In addition, there is a growing interest in CZE on the nano-preparative scale to facilitate collection of fractions for further characterization.

In order to estimate the maximal lumen that allows operation of a capillary without untoward effects of Joule heating, let us first relate the current to the cross-sectional area, A_c, of the capillary as

$$A_c = \frac{1}{4} \cdot \pi d^2 = \frac{I}{\kappa_e E} \quad (17)$$

where d is the inner diameter of the capillary. By combining Eqs. (9) and (17) we obtain the maximum permissible inner diameter, d_{max}, as a function of the relevant operational and capillary parameters

$$d_{max} = \sqrt{\frac{4I}{\pi E e^{\left(A_k - \frac{B}{T}\right)}}} \quad (18)$$

According to Eq. (18), the inner diameter of a capillary is determined by the allowable current, the electric field strength and the temperature dependence of the conductivity. Parameter B for 25 mM sodium phosphate in water–glycerol (65:35,v/v), pH* 7.0, is listed in Table 1. With that data, for four cases with the upper limit of currents set at 20, 50, 75 and 100 μA, the maximal permissible capillary inner diameters as functions of the temperature under otherwise identical conditions were calculated according to Eq. (18). The results are depicted in Fig. 8 and they suggest that in order to use a 180 μm I.D. capillary, even at a current limit of 75 μA, the experiments have to be carried out at subzero temperatures while keeping the capillary length reasonably short.

The feasibility of low temperature in nano-preparative CZE with 180 μm I.D. capillaries is illustrated in Fig. 9 by the separation of four peptides: GF, FG, GGF and FGG. Since one of the main contributing factors to band broadening in capillaries

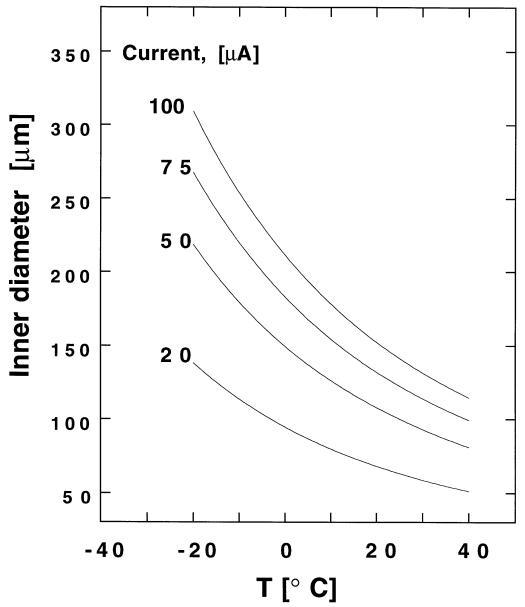

Fig. 8. Plots of the permissible capillary inner diameter according to Eq. (18) against the temperature with the current as the parameter. Data used for calculation: 37 cm long capillary; applied voltage, 20 kV and the viscosity of 25 mM sodium phosphate in water–glycerol (65:35, v/v), pH* 7.0.

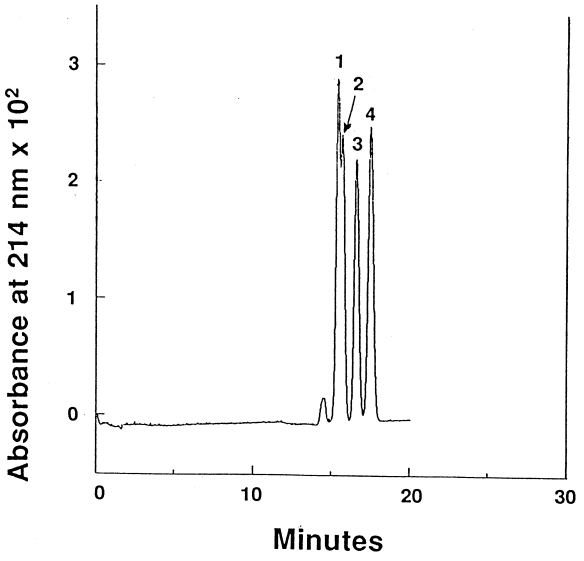

Fig. 9. Electropherograms of peptides obtained at −2°C. Capillary, 37 cm (effective length 30 cm)×180 μm I.D.; 25 mM sodium phosphate in water–glycerol (65:35, v/v), pH* 7.0; applied voltage, 20 kV; current, 105 μA. Sample injected, 32 ng. Peaks: 1=GF; 2=GGF; 3=FG; 4=FGG.

having relatively large lumen is sample injection [26–28], particular attention was paid to keep the length of the sample slug short. Under the experimental conditions investigated here, the total sample amount in the 180 μm I.D. capillary was about 15-times as that in a 50 μm I.D. capillary of the same length. Of course, an alternative approach to avoid the excess Joule heating for a larger diameter capillary at room temperature is to extend the capillary length. Both approaches offer a solution to nano-preparative scale CZE and the ultimate choice will clearly depend on the specific analyte of interest such that the condition of choice would be the one with the optimal resolution.

3.3.4. Effect of buffer concentration in CZE

To suppress electrostatic interactions of the migrants with the capillary inner wall, e.g., in the CZE of small biogenic amines [29] and proteins [30], the use of high buffer concentration would be advantageous lest the high current prohibits. However, the mobility of the background ions decrease upon lowering the temperature and concomitantly the buffering concentration can be increased without an increase in the current.

By combining Eqs. (5) and (7), the temperature dependence of the current is expressed as

$$\frac{I_1}{I_2} = e^{-B\left(\frac{1}{T_1}-\frac{1}{T_2}\right)} \tag{19}$$

where I_1 and I_2 are the respective currents at temperatures T_1 and T_2.

In order to establish the relationship between the buffer concentration and the current, the reference temperature, T_1, was set at 25°C. The current was measured at various concentrations of sodium borate in the BGE at 25°C in a 37 cm long capillary of 50 μm I.D. at a constant applied voltage of 25 kV. The current was calculated according to Eq. (19) in the temperature range from 0 to 50°C under otherwise identical experimental conditions. The results shown in Fig. 10 suggest that in CZE at temperatures near 0°C buffer concentrations as high as 400 m*M* can be used without exceeding the practical limiting current of 70 μA in a 50 μm I.D. capillary. The effect of temperature on the magnitude of EOF has also been examined. Acrylamide was used as the marker for

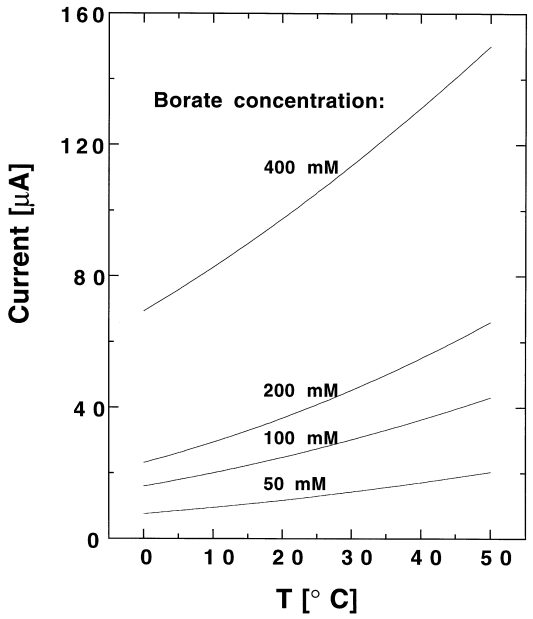

Fig. 10. Plots of the current against the temperature with the borate concentration as the parameter. Capillary, 37 cm (effective length 30 cm)×50 μm I.D.; sodium borate, pH 8.4; applied voltage, 25 kV.

EOF and its mobility was evaluated over a wide range of buffer concentration at 4°C and 25°C. As shown in Fig. 11, plots of μ_{EOF} data against the reciprocal square root of buffer concentrations [15] yield straight lines with a regression coefficient better than 0.99 at concentrations lower than 200 m*M*. However, the data obtained with 400 m*M* buffer at 25°C deviates and this is attributed to changing viscosity due to excess Joule heating at relatively high salt and temperature. This again confirms the earlier finding that the current obtained with the 400 m*M* borate buffer is expected to deviate from theory at temperatures much above 0°C.

As mentioned above, CZE at low temperatures allows the use of relatively high buffer concentrations that have a beneficial effect on the separation. CZE of a mixture containing both small and large molecules was carried out with 100 m*M* and 400 m*M* sodium borate as the BGE at 4°C. The separation with 100 m*M* buffer shown in Fig. 12a has already improved upon decreasing the temperature from 25 (data not shown) to 4°C. By increasing the buffer concentration to 400 m*M*, which is

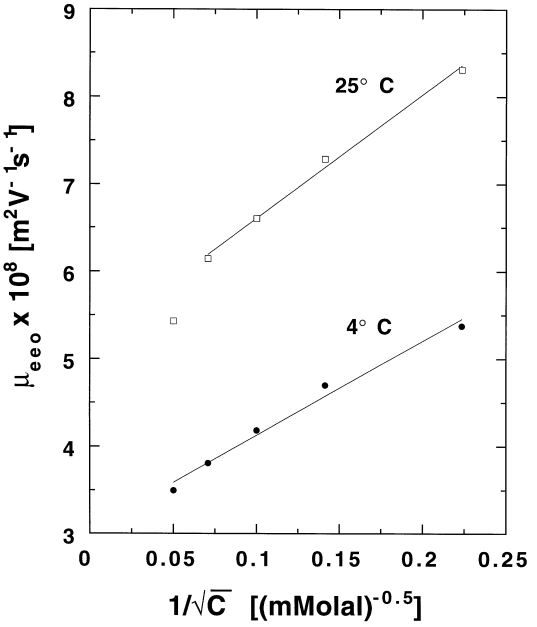

Fig. 11. Plots of the mobility of acrylamide, μ_{EOF}, against the square root of borate concentration at temperatures: (●) 4°C and (□) 25°C. Capillary, 37 cm (effective length 30 cm)×50 μm I.D.; sodium borate, pH 8.4; applied voltage, 25 kV.

possible at 4°C without excess Joule heating problems, the separation is further improved albeit the separation time increased due to the lower EOF velocity as shown by the electropherogram in Fig. 12b. The improvement of the separation at relatively high salt concentration is attributed to the attenuation of electrostatic interactions between the negatively charged capillary inner wall and the positively charged sample components. This can also be concluded by comparing the electrophoretic parameters evaluated from the electropherograms in Fig. 12 and presented in Table 5. The data show the same trend for the dependence of the electrophoretic mobilities and the EOF on the buffer concentration. As the mobilities decrease with increasing salt concentration, the analysis time is slightly increased with the 400 m*M* buffer. As seen in Table 5, the enhancement in the plate efficiency is at least two-fold and the selectivity also increases upon increasing the buffer concentration. Only the peptide glycyl-glycyl-phenylalanine is an exception exhibiting lower selectivity at higher buffer concentration. This behavior may be the results of hydrophobic interactions between the

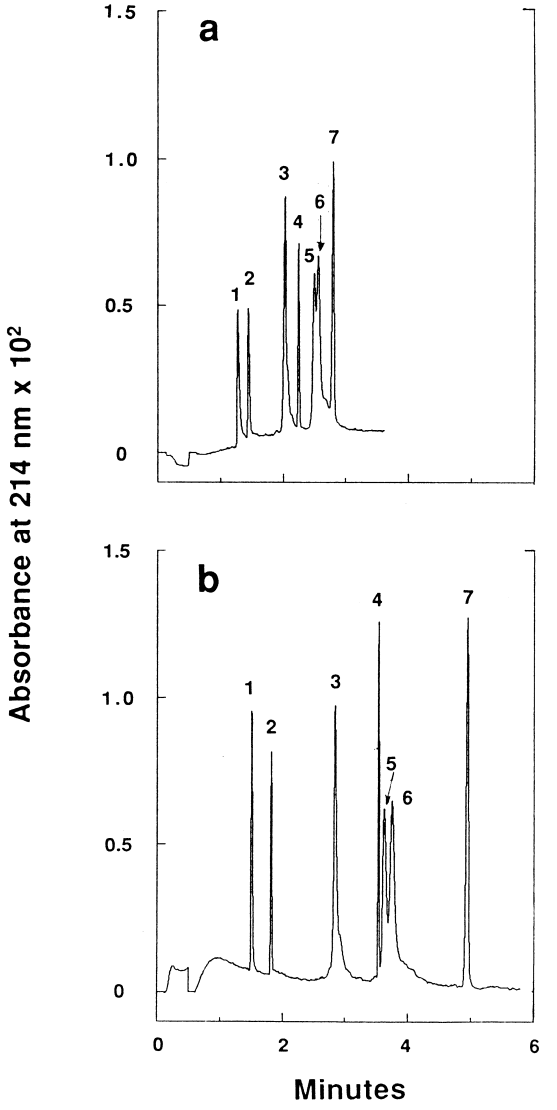

Fig. 12. Electropherograms of an ad hoc mixture obtained with 100 m*M* (a) and 400 m*M* (b) sodium borate, pH 8.4, at 4°C. Capillary, 37 cm (effective length 30 cm)×50 μm I.D.; applied voltage, 25 kV; current, 12 μA (a) and 74 μA (b). Peaks: 1=trimethylphenyl ammonium iodide; 2=ephedrine; 3=myoglobin; 4=GGF; 5=β-lactoglobulin A; 6=β-lactoglobulin B; 7=F.

peptide and the capillary inner wall that are known to be more pronounced at high salt concentrations [31]. Fortunately, hydrophobic interactions are in most cases attenuated upon lowering the temperature [32,33] and this may compensate for the undesirable

Table 5
Effect of the buffer concentration on the electrophoretic mobility, μ, number of theoretical plates, N, and the selectivity of various substances in CZE at 4°C as measured with 100 mM (a) and 400 mM (b) sodium borate buffer, pH 8.4

Peak[a]	Migrant	$\bar{\mu} \cdot 10^8$ ($m^2\ V^{-1}\ s^{-1}$)		N ($\cdot 10^{-3}$)		α[b]		
		100 mM	400 mM	100 mM	400 mM	100 mM	400 mM	Peak pairs
1	TMP[c]	1.91	2.06	5.5	17	1.13	1.21	1, 2
2	Ephedrine	1.23	1.21	14	36	1.40	1.56	2, 3
3	Myoglobin	0.249	0.248	14	27	1.11	1.24	3, 4
4	Glycyl-glycyl-phenylalanine	0.600	0.759	68	210	1.11	1.03	4, 5
5	β-Lactoglobulin A	0.935	0.811	5.3	18	1.03	1.04	5, 6
6	β-Lactoglobulin B	1.01	0.880	6.9	12	1.10	1.32	6, 7
7	*N*-Acetylphenylalanine	1.26	1.36	35	81	–	–	

Capillary, fused-silica 37 cm (effective length 30 cm)×50 μm I.D.; applied voltage, 25 kV; current: (a) 12 μA; (b) 74 μA.
[a] See Fig. 12.
[b] The selectivity, α, is given by the ratio of the electrophoretic mobilities of the two neighboring migrants and by definition $\alpha > 1$.
[c] Trimethylphenyl ammonium iodide.

effect of salt by augmenting hydrophobic interactions.

Facilitating sample stacking [34–37] is another advantage of the high buffer concentration that can be employed in low temperature CZE without high Joule heating. If the buffer concentration in the medium is higher than in the sample solution, then the sample can be concentrated. This may explain the taller and sharper peaks obtained with 400 mM rather than with 100 mM buffer and shown in Fig. 12. In contradistinction, when the buffer concentration in the medium is lower than in the sample solution, the nonuniform conductivity gives rise to significant band dispersion [38,39] with concomitant loss of separation efficiency. This problem may also be overcome by using high buffer concentrations to match the conductivity of the samples, i.e., clinical samples containing phosphate buffer saline, that have usually significantly higher salt concentration than the BGE. Again, low temperature facilitate this approach to enhance separation efficiency.

4. Conclusions

The use of temperatures out of the ordinary in both CZE and HPLC offer improvements over the conventional operation at ambient temperature. It has been shown elsewhere that HPLC has enhanced separation speed and efficiency without complication at elevated temperatures up to 120°C [4]. As illustrated in this report, CZE exhibits enhanced separation efficiency at low temperatures. The improvement in CZE stems mainly from the increased viscosity and the concomitant decrease in molecular diffusion which is the main contributor to peak broadening. As the mobility of the ions in the electrophoretic medium also decrease, capillaries with larger lumen and buffer concentrations higher than usual can be employed. However, due to the prevalent instrument design, axial temperature gradients occur with untoward effects on the control of the process and with loss in the separation efficiency particularly with short column operated far from ambient temperature. Therefore, the prevalent design of CZE instrumentation needed to be altered to facilitate a uniform temperature profiles along the capillary column.

Acknowledgements

This work was supported by grant No. GM 20993 from National Institute of Health, US Public Health Service.

References

[1] Cs. Horváth, B.A. Preiss, S.R. Lipsky, Anal. Chem. 39 (1967) 1422.
[2] Cs. Horváth, S.R. Lipsky, J. Chromatogr. Sci. 7 (1969) 109.

[3] F. Antia, Cs. Horváth, J. Chromatogr. 435 (1988) 1.
[4] H. Chen, Cs. Horváth, Anal. Methods Instrum. 1 (1993) 213.
[5] S. Ma, F. Kálmán, A. Kálmán, F. Thunecke, Cs. Horváth, J. Chromatogr. A 716 (1995) 167.
[6] S. Ma, Cs. Horváth, Electrophoresis 18 (1997) 873.
[7] A. Tiselius, Trans. Faraday Soc. 33 (1937) 524.
[8] C.M. Park, Ann. NY Acad. Sci. 209 (1973) 237.
[9] M. Perrella, A. Heyda, A. Mosca, L. Rossi-Bernardi, Anal. Biochem. 88 (1978) 212.
[10] T. Komuro, C. Yomota, H. Isaka, Chem. Pharm. Bull. 36 (1988) 1218.
[11] M.G. Harrington, T.E. Zewert, Electrophoresis 15 (1994) 195.
[12] G.M. Janini, G.M. Muschik, H.J. Issaq, J. High Resolut. Chromatogr. 17 (1994) 753.
[13] I. Ziegler, D. Scheller, C. Schierle, U. Tielsch, S. Vischer, M. Wiedmann, E. Wirtz, Pharm Rep. 1 (1995) 8.
[14] R.C. Weast, Handbook of Chemistry and Physics, The Chemical Rubber Co., Cleveland, OH, 49th ed., 1968, p. 221.
[15] P.C. Hiemenz, Principles of Colloid and Surface Chemistry, Marcel Dekker, New York, 2nd ed., 1986, p. 677.
[16] P.C. Wankat, Rate-Controlled Separations, Elsevier, New York, 1986, p. 550.
[17] E.N.d.C. Andrade, Nature 125 (1930) 582.
[18] I.N. Levine, Physical Chemistry, McGraw-Hill, New York, 3rd ed., 1988, p. 384.
[19] G.J. Janz, R.P.T. Tomkins, Nonaqueous Electrolytes Handbook, Academic Press, New York, 1972, p. 100.
[20] R.C. Reid, J.M. Prausnitz, B.E. Poling, The Properties of Gases and Liquids, McGraw-Hill, New York, 4th ed., 1987.
[21] D.S. Burgi, K. Salomon, R.-L. Chien, J. Liq. Chromatogr. 14 (1991) 847.
[22] R.J. Nelson, D.S. Burgi, in: J.P. Landers (Ed.), Handbook of Capillary Electrophoresis, CRC Press, Ann Arbor, MI, 1994, p. 549.
[23] J.H. Knox, K.A. McCormack, Chromatographia 38 (1994) 207.
[24] J.C. Giddings, Sep. Sci. 4 (1969) 181.
[25] J.C. Giddings, J. Chromatogr. 395 (1987) 19.
[26] H.H. Lauer, D. McManigill, Trends Anal. Chem. 3 (1986) 11.
[27] E. Grushka and R.M. McCormick, J. Chromatogr., 471 (1989) 421.
[28] S.L. Delinger, J.M. Davis, Anal. Chem. 64 (1992) 1947.
[29] S. Fanali, J. Chromatogr. 474 (1989) 441.
[30] J.S. Green, J.W. Jorgenson, J. Chromatogr. 478 (1989) 63.
[31] W.R. Melander, Z.E. Rassi, Cs. Horváth, J. Chromatogr. 469 (1989) 3.
[32] C. Tanford, The Hydrophobic Effect: Formation of Micells and Biological Membranes, Wiley-Interscience, New York, 1980.
[33] D. Haidacher, A. Vailaya, Cs. Horváth, Proc. Natl. Acad. Sci. 93 (1996) 2290.
[34] F.M. Everaerts, T.P.E.M. Verheggen, F.E.P. Mikkers, J. Chromatogr. 169 (1979) 11.
[35] S. Hjertén, Electrophoresis 11 (1990) 665.
[36] A. Vinther, H. Søeberg, J. Chromatogr. 559 (1991) 3.
[37] D.S. Burgi, R.-L. Chien, Anal. Chem. 63 (1991) 2042.
[38] D. Schmalzing, W. Nashabeh, M. Fuchs, Clin. Chem. 41 (1995) 1403.
[39] D. Schmalzing, W. Nashabeh, X.-W. Yao, R. Mhatre, F.E. Regnier, N.B. Afeyan, M. Fuchs, Anal. Chem. 67 (1995) 606.